Model-based Estimation of Vertebrae from Uncalibrated Bi-Planar XRays

Brendan McCane

Department of Computer Science
University of Otago
Email: mccanecs.otago.ac.nz

Abstract—This paper presents a method and preliminary study for estimating the location of vertebrae from uncalibrated bi-planar radiographs. The method uses the axis/angle representation of rotations and exact analytic derivatives for optimising the objective function. Multiple vertebral models are incorporated in a single procedure. Results are shown on both real data in vivo and on simulated data. No ground truth for the real data is available, but sensible results are produced by the method in comparison with a method using numeric derivatives. Simulation results show that the method is robust to Gaussian errors in the landmarks and degrades gracefully as these errors increase.

I. Introduction

In the diagnosis and treatment of pediatric scoliosis patients, the analysis of the three-dimensional (3D) structure of the spine is extremely important. Ideally, CT-scans would be used to estimate this structure, but because of the need for frequent scans (every 6 months over several years), such scans would result in an unacceptable radiation exposure risk. As a consequence, most specialists employ approximately orthogonal bi-planar radiographs to track progress without any explicit 3D reconstruction or measurement [1].

This paper presents a preliminary study introducing a new method for 3D model-based estimation of vertebrae from uncalibrated bi-planar radiographs. Although calibrated images are relatively straightforward to obtain, any such technique could not be applied to the very large number of clinical images already in existence. Several methods have been proposed to tackle the problem of 3D estimation from bi-planar images [2], [3], [4], [5], [6], [7], [8], [9], [10]. However, most of these techniques require calibrated images [2], [3], [5], [6], [7], [9], [10]. Those that do not require a separate calibration procedure or make use of some information from a known calibration object [4], [8], and are therefore not valid for use

on historical data. More recent work in [11], [12] use anatomical landmarks only for self-calibration as in the work presented here. However, in that work, it appears that numeric derivatives are used and consequently "The self-calibration algorithm is very sensitive to the quality of the input data that is acquired ..." [11].

This paper presents a new method for the reconstruction of vertebral position from two approximately orthogonal bi-planar uncalibrated radiographs. The method takes a different approach to previous solutions: no calibration object is needed; non-corresponding image points are used; multiple vertebral models are integrated into the self-calibration procedure; an axis/angle vector representation of rotation is used; exact analytic derivatives are derived for use in the optimisation procedure. The use of analytic derivatives and the axis/angle axis representation results in a method that is robust to landmark localisation errors.

A weakness of the current work is that it assumes that an appropriate 3D model of the vertebrae is given and that corresponding landmarks on the vertebrae and in the images are likewise given. This is in contrast to some recent work that attempts to automatically locate vertebrae in radiographic images [13], [14], [10]. Automatic localisation and correspondence has not been attempted here because the focus is on developing a method for uncalibrated cameras.

II. Problem Statement and Representation

The problem is to calculate the 3D position of each vertebra from a lateral and anterior-posterior (AP) radiograph taken in an uncalibrated setting. It is assumed that the world coordinate origin is aligned with the lateral image and that the same acquisition parameters are used for each image (same focal length). Inputs to the algorithm include the
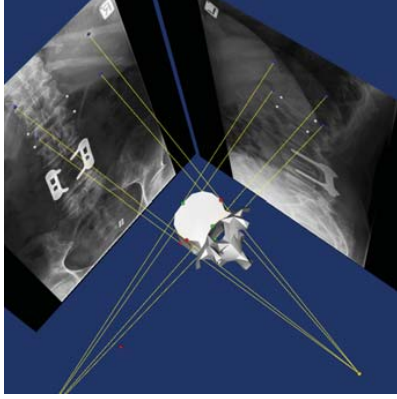
Fig. 1. The imaging setup. It is assumed that an approximate vertebra model with identified landmarks is available. Projected landmarks on the images are also given. The goal is to adjust imaging parameters and model transformation parameters to minimise the distance between identified image points and projected landmark points.

model coordinates of each vertebra, $\mathbf{x_{nj}}$, and corresponding landmark coordinates on the images, $\mathbf{l_{nj}}$ and $\mathbf{ap_{nj}}$. The image acquisition parameters to estimate are:

$\mathbf{c_p}$ Centre of projection (3 parameters). $\mathbf{c_p} = [c_x, c_y, f]$, where c_x, c_y are the image coordinates of the centre of projection, and f is the focal length.

$\mathbf{t_{ap}}$ axis/angle for AP image (3 parameters), where $\frac{\mathbf{t_{ap}}}{|\mathbf{t_{ap}}|}$ is the axis of rotation, and $|\mathbf{t_{ap}}|$ is the angle of rotation. This is an exponential map representation of rotations [15].

$\mathbf{d_{ap}}$ translation vector for AP image (3 parameters).

For each vertebra under consideration, there is a need to estimate the following parameters:

$\mathbf{t_n}$ axis/angle vector for vertebra n (3 parameters)

$\mathbf{S_n}$ scale parameters for vertebra n (3 parameters, one for each dimension independently). $\mathbf{S_n}$ is represented as a diagonal 3-matrix.

$\mathbf{d_n}$ translation vector for vertebra n (3 parameters).

The imaging setup is shown in Figure 1.

A. Model Transformations

Given coordinates of the model in model space, $\mathbf{x_{nj}}$, for vertebra n and landmark coordinate j,

the model transformation into world coordinates is given by:

$$\mathbf{w_{nj}} = \mathbf{S_n} \exp([\mathbf{t}]_\times)\mathbf{x_{nj}} + \mathbf{d_n}, \qquad (1)$$

where $\mathbf{w_{nj}}$ are the world coordinates, and $\exp([\mathbf{t}]_\times)$ is the exponential map converting the axis/angle vector representation into a rotation matrix [16, p.583-585].

B. Camera Projections

For the lateral image, projection is straightforward:

$$\hat{\mathbf{l}}_{\mathbf{nj}} = \frac{f(\mathbf{w_{nj}} - \mathbf{c_p})}{(\mathbf{w_{nj}} - \mathbf{c_p})[z]} + \mathbf{c_p}, \qquad (2)$$

where the notation $\mathbf{x}[z]$ indicates the z-coordinate of a 3-vector, and the hat notation indicates an estimated or reprojected point.

For the AP image, the projection is more difficult. Rather than directly calculate the projection transformation onto an arbitrary plane, it is simpler to inverse transform the world coordinates into the coordinate system of the plane, then perform the simple projection transformation:

$$\mathbf{w_{nj-ap}} = \exp([-\mathbf{t_{ap}}]_\times)(\mathbf{w_{nj}} - \mathbf{d_{ap}}) \quad (3)$$

$$\hat{\mathbf{ap}}_{\mathbf{nj}} = \frac{f(\mathbf{w_{nj-ap}} - \mathbf{c_p})}{(\mathbf{w_{nj-ap}} - \mathbf{c_p})[z]} + \mathbf{c_p} \qquad (4)$$

C. Minimisation Procedure

The equation to minimise is:

$$F_{L,N,M}(\mathbf{S}_{1:L}, \mathbf{t}_{1:L}, \mathbf{d}_{1:L}, \mathbf{c_P}, \mathbf{t_{ap}}, \mathbf{d_{ap}}) =$$

$$\sum_{n=1}^{L} \left[\sum_{j=1}^{N} ||\mathbf{l_{nj}} - \hat{\mathbf{l}}_{\mathbf{nj}}||^2 + \sum_{j=N}^{N+M} ||\mathbf{ap_{nj}} - \hat{\mathbf{ap}}_{\mathbf{nj}}||^2 \right] \quad (5)$$
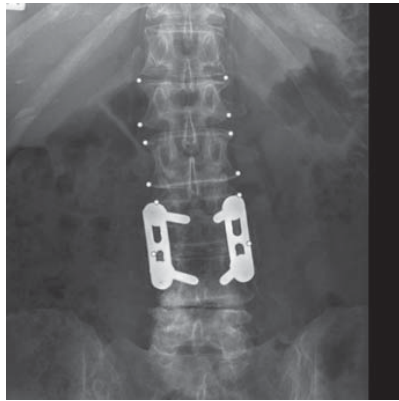
where, L is the number of vertebrae, N, M are the number of correspondences for the lateral and AP image respectively. The total number of free parameters are:

$$N_f = 9L + 9 = 9(L+1). \qquad (6)$$

Therefore the minimum number of correspondences needed is $9(L+1)/2$ (each correspondence gives two equations).

(a) The Lateral Image

(b) The Anterior-Posterior Image

Fig. 2.   Landmarks

For this paper, eight correspondences per vertebra are used - four each for the lateral and AP image. Three vertebra are used: L1-L3. The landmarks chosen are the four corners of the vertebra body as seen in each image. The landmarks are shown in Figure 2. The corner landmarks are standard anatomical landmarks [17], [18]. Note that landmarks obscured by the vertebral fusion device for Patient 1 have been estimated based on nearby image information.

Analytic derivatives increase the chance of numeric optimisation procedures successfully converging on a valid minima. Although numeric derivatives can be computed, they tend to produce less satisfactory results. Instead, direct analytic derivatives have been used in this paper. Unfortunately, the derivatives are not simple and there is no room to include them in the paper. The Sage system [19] was used to generate the derivatives (via Maxima [20]), and python code

	Patient 1	Patient 2
Starting Error	110029	1153434
Analytic Gradient	1980	3898
Numeric Gradient	25521	29768

TABLE I
SUM SQUARED ERROR (PIXELS) FOR EACH PATIENT. THE
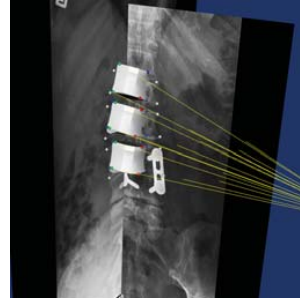ERROR REPORTED IS CALCULATED FROM EQUATION 5.

Fig. 3.   The initial configuration.

for computing the derivatives was generated directly from the Sage results. This methodology reduced the likelihood of errors (the largest derivative has several hundred terms) and made calculation of analytic derivatives feasible. Note that the analytic derivatives used here are exact rather than the approximate derivative usually used for these sorts of applications for small rotation angles [21, p. 39].

The `scipy.optimize.leastsq` (Levenberg-Marquardt optimisation) function from [22] has been used to find the optimal parameters both with and without explicit gradient computations.

III. Results

A. Real Data

Currently, there is available only a very small set of real data (two image pairs) with no ground truth available. Nevertheless, even this minimal set provides a useful comparison between analytic and numeric derivative schemes. Figure 3 shows the starting position for one of the image pairs, Figure 4 shows the optimisation result using analytic derivatives, and Figure 5 shows the results using numeric derivatives, both for patient 1. Figure 6 and 7 show the corresponding images for patient 2. Table I shows the final mean-squared error for the projected versus the actual landmarks for both sets of image pairs.
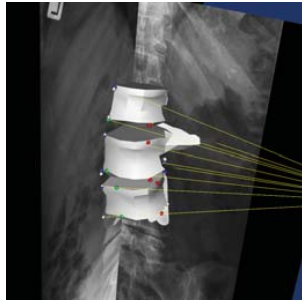
Fig. 4.   Result with analytic derivatives for patient 1.
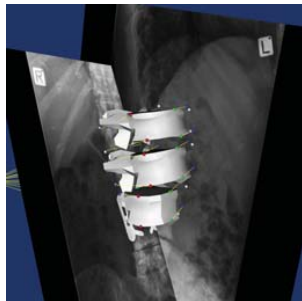

Fig. 5.   Result with numeric derivatives for patient 1.
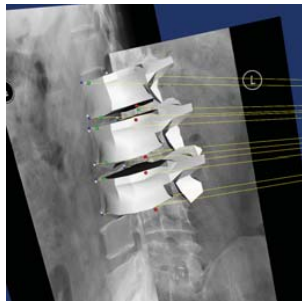

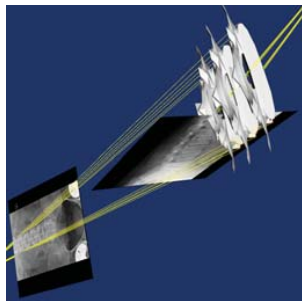Fig. 6.   Result with analytic derivatives for patient 2.

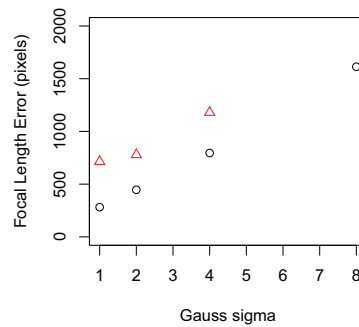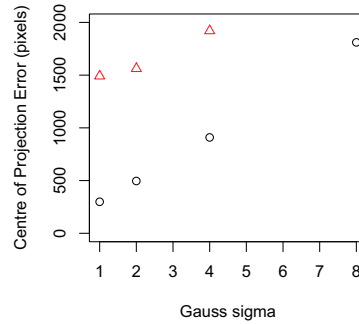Fig. 7.   Result with numeric derivatives for patient 2.

Fig. 8.   Centre Of Projection: Simulation results for analytic (circles) versus numeric (triangles) gradients.

B. Simulation Results

To test the hypothesis that the analytic derivatives produce robust parameter estimates, the following experiment was conducted. A particular model configuration of vertebrae and image planes was chosen and the model landmarks were projected to the images and stored as ground truth landmarks. The ground truth landmarks were then used to generate new landmark configurations by adding isotropic Gaussian noise to each coordinate. Scale differences are reported independently for each dimension, translation differences are reported as a single distance (including centre of projection), and rotation differences are reported in two components - angle between rotation axes, and angle difference between rotation angles. Isotropic Gaussian noise of $\sigma = \{1.0, 2.0, 4.0, 8.0\}$ was added to the landmarks in 100 independent trials For each noise level of $\sigma = \{1.0, 2.0, 4.0, 8.0\}$, 100 independent new image landmark configurations were generated and the optimisation procedure was applied to each new pair of configurations. Figures 8, 9 and 10 show the resulting errors for the analytic and numeric gradients respectively.
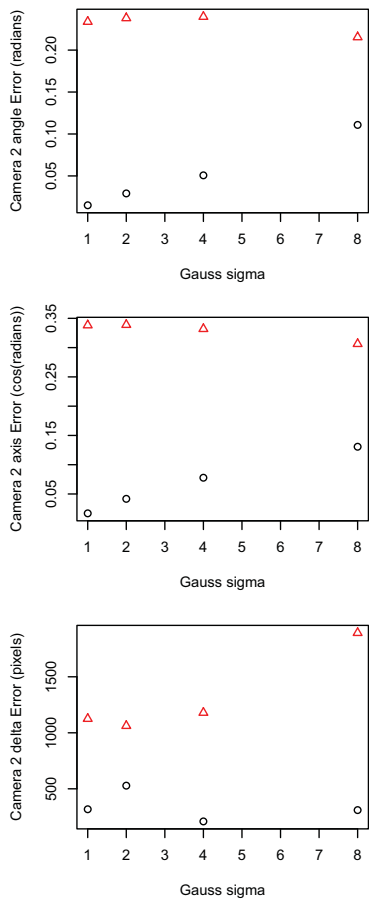
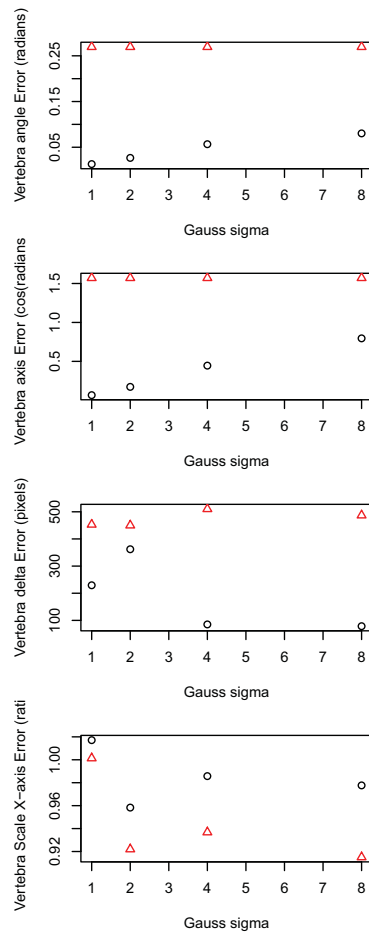Fig. 9. Camera 2: Simulation results for analytic (circles) versus numeric (triangles) gradients.

Fig. 10. Vertebra L1: Simulation results for analytic (circles) versus numeric (triangles) gradients.

IV. Conclusion

In this paper, a method for estimating the 3D location of vertebrae from two approximately orthogonal uncalibrated images has been presented. Although much of the derivation is standard, it has been shown that the use of analytic derivatives is (not surprisingly) superior to the use of numeric approximations. In vivo results from two patients shows that the method produces sensible configurations, although no ground truth data was available. Simulation studies have shown that the method is robust to Gaussian errors in landmark estimation and that the performance degrades gracefully even in the presence of quite large errors.

This work is still quite preliminary and there are many potential avenues for extension. The most important task will be to develop a set of real data with ground truth available so that a more thorough evaluation can be performed. It would be useful to compare the current method using full analytic derivatives with the more usual analytic approximations used in the literature [21, p. 39]. Similarly, more efficient optimisers such as sparse Levenberg-Marquardt should be compared. Currently no attempt at automatic detection of landmarks has been attempted and this is an obvious and necessary extension for use in clinical practice. Also, a limited form of vertebra deformation (independent scaling along each axis) has been used here. For diseased spines, especially those suffering from scoliosis, more general vertebra deformation is likely to be needed for accurate recovery of position.

References

[1] B. Hodgson, "Orthopaedic surgeon," Personal Communication, 2010.

[2] J. Dansereau and I. Stokes, "Measurements of the three-dimensional shape of the rib cage," *Journal of biomechanics*, vol. 21, no. 11, pp. 893–901, 1988.

[3] Y. Petit, J. Dansereau, H. Labelle, and J. De Guise, "Estimation of 3d location and orientation of human vertebral facet joints from standing digital radiographs," *Medical and Biological Engineering and Computing*, vol. 36, no. 4, pp. 389–394, 1998.

[4] F. Cheriet, J. Dansereau, Y. Petit, C. Aubin, H. Labelle, and J. De Guise, "Towards the self-calibration of a multiview radiographic imaging system for the 3d reconstruction of the human spine and rib cage," *International Journal of Pattern Recognition and Artificial Intelligence*, vol. 13, no. 5, pp. 761–779, 1999.

[5] D. Mitton, C. Landry, S. Veron, W. Skalli, F. Lavaste, and J. De Guise, "3d reconstruction method from bi-planar radiography using non-stereocorresponding points and elastic deformable meshes," *Medical and Biological Engineering and Computing*, vol. 38, no. 2, pp. 133–139, 2000.

[6] R. Dumas, A. Le Bras, N. Champain, M. Savidan, D. Mitton, G. Kalifa, J. Steib, J. de Guise, and W. Skalli, "Validation of the relative 3d orientation of vertebrae reconstructed by bi-planar radiography," *Medical engineering & physics*, vol. 26, no. 5, pp. 415–422, 2004.

[7] V. Pomero, D. Mitton, S. Laporte, J. de Guise, and W. Skalli, "Fast accurate stereoradiographic 3d-reconstruction of the spine using a combined geometric and statistic model," *Clinical Biomechanics*, vol. 19, no. 3, pp. 240–247, 2004.

[8] S. Kadoury, F. Cheriet, C. Laporte, and H. Labelle, "A versatile 3d reconstruction system of the spine and pelvis for clinical assessment of spinal deformities," *Medical and Biological Engineering and Computing*, vol. 45, no. 6, pp. 591–602, 2007.

[9] S. Bertrand, S. Laporte, S. Parent, W. Skalli, and D. Mitton, "Three-dimensional reconstruction of the rib cage from biplanar radiography," *IRBM*, vol. 29, no. 4, pp. 278–286, 2008.

[10] L. Humbert, J. De Guise, B. Aubert, B. Godbout, and W. Skalli, "3d reconstruction of the spine from biplanar x-rays using parametric models based on transversal and longitudinal inferences," *Medical engineering & physics*, vol. 31, no. 6, pp. 681–687, 2009.

[11] S. Kadoury, F. Cheriet, J. Dansereau, and H. Labelle, "Three-dimensional reconstruction of the scoliotic spine and pelvis from uncalibrated biplanar x-ray images," *Journal of spinal disorders & techniques*, vol. 20, no. 2, pp. 160–167, 2007.

[12] S. Kadoury, F. Cheriet, and H. Labelle, "Self-calibration of biplanar radiographic images through geometric spine shape descriptors," *Biomedical Engineering, IEEE Transactions on*, vol. 57, no. 7, pp. 1663–1675, 2010.

[13] S. Benameur, M. Mignotte, S. Parent, H. Labelle, W. Skalli, and J. de Guise, "3d/2d registration and segmentation of scoliotic vertebrae using statistical models," *Computerized Medical Imaging and Graphics*, vol. 27, no. 5, pp. 321–337, 2003.

[14] G. Zheng and L. Nolte, "Surface reconstruction of bone from x-ray images and point distribution model incorporating a novel method for 2d-3d correspondence," in *IEEE Conference on Computer Vision and Pattern Recognition*. IEEE Computer Society, 2006.

[15] F. Grassia, "Practical parameterization of rotations using the exponential map," *Journal of graphics tools*, vol. 3, pp. 29–48, 1998.

[16] R. Hartley and A. Zisserman, *Multiple view geometry in computer vision*. Cambridge Univ Press, 2003.

[17] M. J. Pearcy and N. Bogduk, "Instantaneous aces of rotation of the lumbar invertebral joints," *Spine*, vol. 13, no. 9, pp. 1033–1041, 1988.

[18] S. Harvey and D. Hukins, "Measurement of lumbar spinal flexion-extension kinematics from lateral radiographs: simulation of the effects of out-of-plane movement and errors in reference point placement," *Medical Engineering and Physics*, vol. 20, pp. 403–409, 1998.

[19] W. Stein *et al.*, *Sage Mathematics Software (Version 4.5)*, The Sage Development Team, 2010, http://www.sagemath.org.

[20] *Maxima, a Computer Algebra System, Version 5.18.1*, 2009, http://maxima.sourceforge.net/.

[21] R. Szeliski, *Computer vision: Algorithms and applications*. Springer-Verlag London, 2011.

[22] E. Jones, T. Oliphant, P. Peterson *et al.*, "SciPy: Open source scientific tools for Python," 2001–. [Online]. Available: http://www.scipy.org/